

of proteins and other macromolecules. Continued advances in membrane science and manufacture and engineering improvements to modules and systems will allow a greater penetration of this technology in a variety of industries in the future.

See also: II/Membrane Separations: Filtration; Micro-filtration.

Further Reading

- Bhave RR (ed.) (1991) *Inorganic Membranes. Synthesis, Characteristics and Applications*. New York: Van Nostrand Reinhold.
- Cheryan M (1998) *Ultrafiltration and Microfiltration Handbook*. Lancaster, PA: Technomic.
- Cheryan M and Alvarez J (1995) Membranes in food processing. In: Noble RD and Stern SA (eds) *Membrane*

- Separations. Technology, Principles and Applications*, p. 415. Amsterdam: Elsevier.
- Cheryan M and Rajagopalan N (1998) Membrane treatment of oily streams. Wastewater treatment and waste reduction. *Journal of Membrane Science* 151: 15–38.
- Ho WSW and Sirkar KK (eds) (1992) *Membrane Handbook*. New York: Chapman and Hall.
- Hsieh HP (1996) *Inorganic Membranes for Separation and Reaction*. Amsterdam: Elsevier.
- Lloyd DR (ed.) (1985) *Materials Science of Synthetic Membranes*. Washington, DC: American Chemical Society.
- Matsuura T (1994) *Synthetic Membranes and Membrane Separation Processes*. Boca Raton, FL: CRC Press.
- Mulder M (1991) *Basic Principles of Membrane Technology*. Norwell, MA: Kluwer Academic Publishers.
- Singh N and Cheryan M (1998) Membrane technology in corn refining and bio-products processing. *Starch/Stärke* 50: 16–23.

PARTICLE SIZE SEPARATION: Electric Fields in Field Flow Fractionation

See II/PARTICLE SIZE SEPARATION/Field Flow Fractionation: Electric Fields

PARTICLE SIZE SEPARATION



Electrostatic Precipitation

J. J. Harwood, Tennessee Technological University, Cookeville, TN, USA

Copyright © 2000 Academic Press

Introduction

Electrostatic precipitators (ESPs) are the most commonly used devices for the removal of fine particles in exhaust from industrial and utility processes. Wire-plate ESPs consist of three or more sections of arrays of large (e.g., 15 m × 5 m), grounded metal collector plates between which are situated wire or other narrow, high voltage electrodes (Figure 1). Less commonly, a wire-cylinder electrode configuration is used. Particles entering the first section are quickly charged by ions generated by the plasma coronas around the wires. (Current does pass between the

electrodes, hence the term ‘electrostatic’ is not really accurate, but indicates the small current-to-electrode area.) The charged particles are drawn toward and deposit upon the collector plates, which are periodically cleaned by mechanical ‘rapping’. This method is very efficient in removing particles in the 1–>10 µm range. The most common use of ESPs is in control of exhaust from coal combustion utilities. Precipitators are also used in the cement, ore smelting, steel production, pulp and paper manufacturing, and chemical processing industries, and in waste combustion utilities. Small units are used in cleaning domestic and workplace air, and have been considered for use in animal production facilities.

M. Holfield first demonstrated the removal of particles by electrostatic charging in 1820. Holfield showed that tobacco smoke can be cleared in a bottle by applying a spark-producing voltage to a pointed electrode inserted in the bottle. In 1850, C. F. Guitard observed that a steady corona discharge is effective in dissipating smoke. Sir Oliver Lodge first attempted

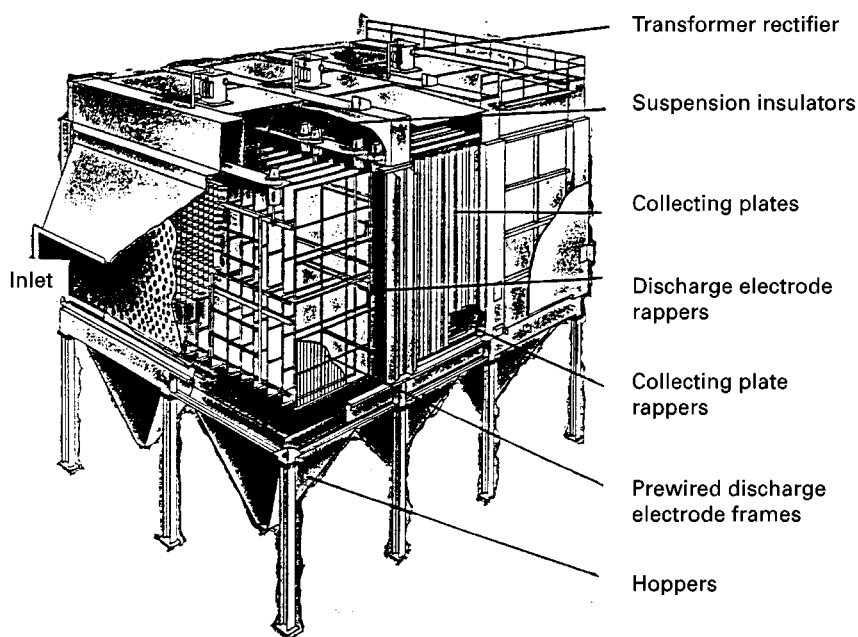


Figure 1 Rigid frame electrostatic precipitator. (Reproduced with permission. Copyright Wheelabrator Air Pollution Control Inc.)

the commercial application of this phenomenon by constructing an electrostatic precipitator to control fumes at a lead smelter. Unfortunately, lead oxide is too resistive to allow sufficient particle charging with a constant DC discharge, and the application failed. The first successful commercial application of electrostatic precipitation was by F. G. Cottrell, who designed an ESP to remove acid mist from sulfuric acid plants. Cottrell facilitated the establishment of the technique by developing the first suitable high-voltage power supplies. ESP particle control became widely used between 1910 and 1930.

Removal of small particles from gas streams is important for process, health, and environmental reasons. Centrifugal separators are used to remove particles larger than $10\ \mu\text{m}$; fabric filter 'baghouses' are used to remove finer particles and constitute a viable alternative to ESPs. Capital costs are similar for baghouses and ESPs; however, maintenance, including energy cost, is lower with ESP units.

The increased control of sulfur and nitrogen oxides in the 1970s, and recent calls for the control of very fine particles, challenge scientists and designers concerned with the ESP technique. Use of low sulfur coal reduces fly ash resistivity below that appropriate for conventional ESP operation. Treatment by the addition of limestone to coal increases the particle load on precipitators. Conventional precipitators do not efficiently remove submicron particles. As will be discussed in this chapter, researchers are developing means of adapting ESP design and opera-

tion to meet the challenges of improved environmental control.

Characteristics of Fly Ash

Hart *et al.* recently performed a comprehensive investigation of the composition and mineralogy of fly ash from three utility boilers. Using instrumental neutron activation analysis and X-ray fluorescence spectroscopy, they found Si, Al, Fe and Ca to account for more than 90% of major elements from all three boilers. Scanning electron microscopy with energy dispersive spectroscopy revealed successive ESP ashes to be composed mainly of spherical particles which decrease in average diameter with increasing distance from the boiler. Concentrations of As, Co, Cr, Ni, Mo and Sb increased from bottom ash through the sequence of ESP ashes. These trace elements are volatilized and transported to cooler regions, where they condense or are adsorbed onto fly ash particles. The major fly ash mineral phase found by these and other researchers is quartz (SiO_2) with magnetite (Fe_3O_4), anhydrite (CaSO_4), and mullite ($\text{Al}_6\text{Si}_2\text{O}_{13}$) among other minerals commonly present.

Resistivity (ρ) is the most important property of material to be collected by an ESP. The optimum range of resistivity is 10^4 – $10^{11}\ \Omega\text{-cm}$. On collection, low resistivity particles ($\rho \leq 10^3\ \Omega\text{-cm}$) release charge to the collector plate and may be re-entrained. Particles with $\rho > 10^{11}\ \Omega\text{-cm}$ insulate the collector plate, ultimately producing a sufficiently large electric field

within the dust layer to cause a counterproductive 'back corona'.

Two types of resistivity may be important in particle collection in an ESP. Ions collected at the surface of particles control 'surface resistivity', which dominates at temperatures below 250°C. As indicated in Figure 2, particle resistivity first increases with temperature, then decreases. Removal of the surface film (adsorbed water) by heating *in vacuo* at 360°C eliminates this initial increase in resistivity. Above 200°C, removal of adsorbed material no longer affects resistivity, and at higher temperatures resistivity is attributed to ions in the bulk of the particles,

'volume resistivity'. Both types of resistivity are primarily functions of Na^+ and Li^+ ion concentrations, and in some cases K^+ and I^- ions.

Two aspects of the ρ - T relationship affect ESP collection efficiency. First, the maximum resistivity of fly ash occurs within the range of temperature at which ESPs are commonly operated, 130–180°C. Second, SO_3 , produced from sulfur in coal, adsorbs onto the fly ash particles and has traditionally been responsible for lowering the resistivity of the particles to the optimum range for collection. Present use of low sulfur coals (<1% S) leads to inadequate collection.

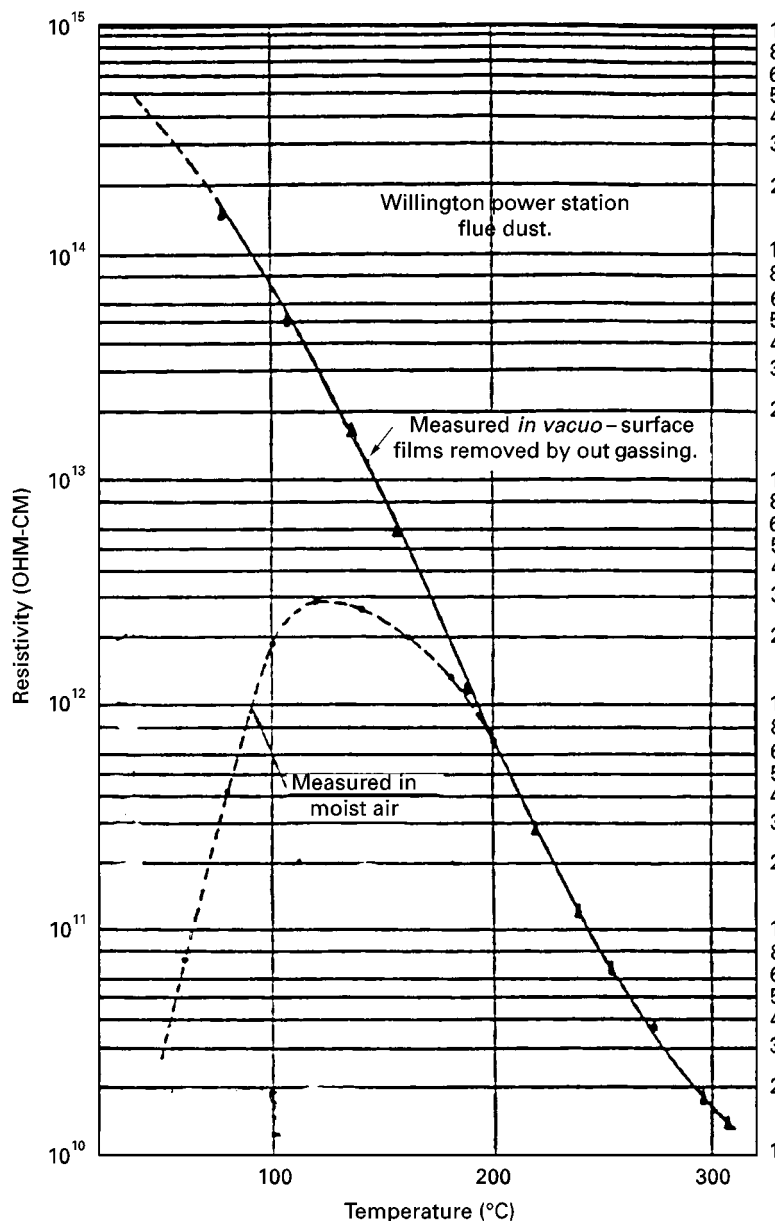


Figure 2 Effect of surface film resistivity on flue-dust resistivity. (Reproduced with permission from Busby HGT and Darby K (1963) *Journal of the Institute of Fuel* 36(268): 184. Copyright The Institute of Fuel).

Operation at non-optimal temperature can be avoided by lowering the temperature, but this requires energy input to a cooling device, and also can lead to difficulties with corrosion due to condensation. The temperature of the exhaust is normally cooled by heat exchange in an air pre-heater prior to injection into the precipitator, hence the name 'cold-side' precipitator. 'Hot-side' precipitators operate at temperatures as high as 370°C; resistivity is often reduced to a desirable level of $2 \times 10^{10} \Omega\text{-cm}$ at above 315°C. However, difficulties are encountered with the greater volume of the hot gas, and these units require more careful construction.

More commonly, resistivity of high-resistance ash is lowered by chemical conditioning.

Theoretical and Practical Aspects of Electrostatic Precipitation

Charging of Particles

The corona surrounding a discharge electrode of an ESP is a gas plasma of electrons and cations. The cations are drawn into the electrode, which is biased negative. The electrons are repelled into the interelectrode space where, within one centimetre travel, they ionize gas particles. These gas particles are drawn toward the grounded collector electrodes. On the way, many of them collide with and attach to the particles to be collected, charging them. The charged particles are then drawn towards the collector electrodes. This particle charging is efficient. Typical charging time is 5 ms; typical residence time in an ESP is 2–5 s.

Charging processes are of two types: field charging, where ions moving with the electric field charge the particles, and diffusion charging, where charging is due to collision with ions moving with random thermal motion. The types are distinguished to facilitate mathematical description. Field charging is dominant in charging particles with radius (a) greater than $0.5 \mu\text{m}$; diffusion charging is dominant with $< 0.2 \mu\text{m}$ particles. Both mechanisms are important in the intermediate size range.

The charge on an ion at time t ($q(t)$) resulting from field charging, derived by Pauthenier and Moreau-Hanot is:

$$q(t) = 12 \frac{\kappa}{\kappa + 2} \pi \epsilon_0 a^2 E_0 \frac{t}{t + \tau}$$

where κ is the relative dielectric constant; ϵ_0 is the permittivity of free space ($\text{C}^2 \text{N}^{-1} \text{m}^{-1}$); a is the particle radius (m); E_0 is the electric field (V m^{-1}); t is the

time (s) and:

$$\tau = 4\epsilon_0/N_0eb$$

where N_0 is the number density of particles (m^{-3}); e is the electronic charge (C); b is the ion mobility ($\text{m}^2 \text{s}^{-1} \text{V}^{-1}$). (This and other formulae are in the form presented in Oglesby and Nichols (see Further Reading.) The corresponding expression for diffusion charging presented by White is:

$$q(t) = \frac{akT}{e} \ln \left(1 + \frac{\pi av N_0 e^2 t}{kT} \right)$$

where k is the Boltzmann's constant (J K^{-1}); v is the rms thermal velocity of ions (m s^{-1}); T is the absolute temperature (K).

Smith and McDonald derived an expression for combined diffusion and particle charging. They divided the surface of a particle being charged into three regions: region I, where the electric field of the particle and that within the ESP duct intersect, sweeping ions onto the particle surface; region II, where the radial component of the electric field of the particle dominates; and region III, where the electric field of the particle and duct are in the same direction, sweeping ions away from the particle. Giving the electric field about the particle, E_r , as:

$$E_r = E_0 \cos \theta \left(1 + 2 \frac{\kappa - 1}{\kappa + 2} \frac{a^3}{r^3} \right) - \frac{ne}{4\pi\epsilon_0 r^2}$$

where E_r is the radial component of electric field (V m^{-1}); E_0 is the external field (V m^{-1}); r is the radial distance to point of interest (m); θ is the azimuth angle measured from the z axis (toward the discharge electrode) (rad); ne is the particle charge (C); these researchers produced a combined charging rate equation:

$$\begin{aligned} \frac{dq}{dt} &= \frac{dq}{dt_I} + \frac{dq}{dt_{II}} + \frac{dq}{dt_{III}} \\ &= (N_0 A n_s e^2 / 4\epsilon_0) \left(1 - \frac{n}{n_s} \right)^2 \\ &\quad + \frac{e\pi a^2 v N_0}{2} \int_{\theta_0}^{\pi/2} \exp \left[- \left(\frac{ne^2(r_0 - a)}{4\pi\epsilon_0 k T a r_0} \right. \right. \\ &\quad \left. \left. + \frac{[3ar_0^2 - r_0^3(\kappa + 2) + a^3(\kappa - 1)]eE_0 \cos \theta}{k T r_0^2(\kappa + 2)} \right) \right] \sin \theta d\theta \\ &\quad + \frac{e\pi a^2 v N_0}{2} \exp(-ne^2/4\pi\epsilon_0 a k T) \end{aligned}$$

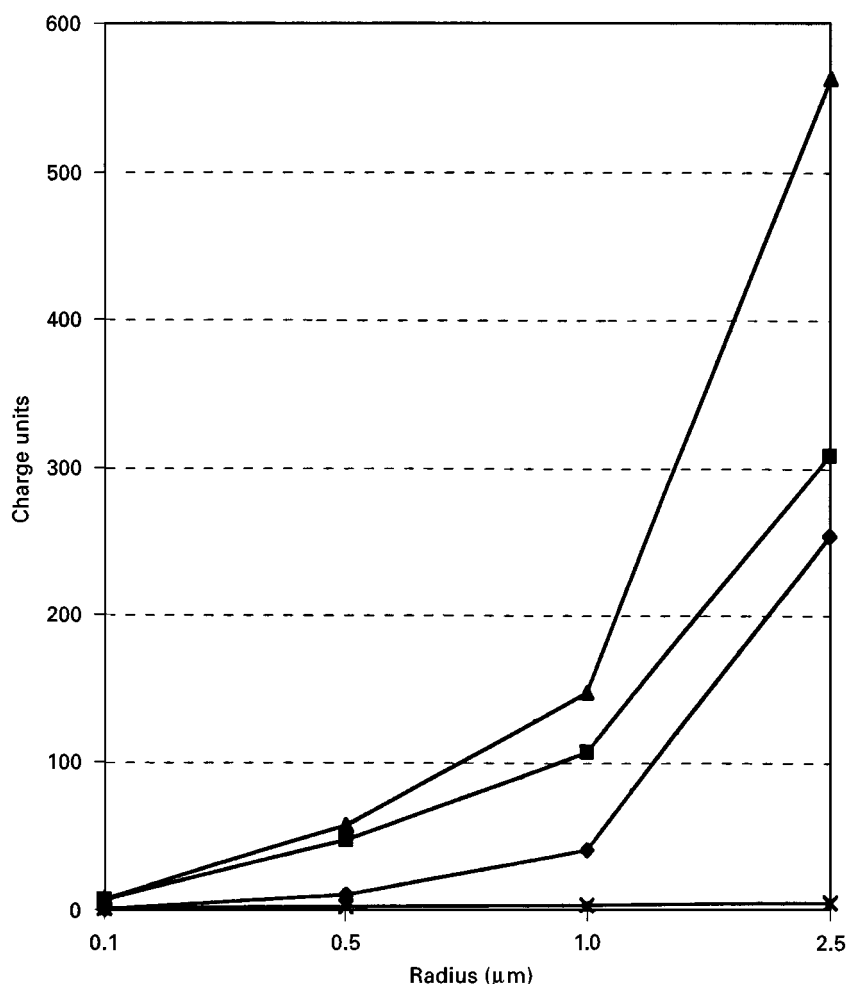


Figure 3 Modes of particle charging. —♦—, field charging; —■—, diffusion charging; —▲—, total charge; —×—, Boltzman charge AC. (Data from Kanazawa *et al.* (1993) *Journal of Electrostatics* 29: 193. Copyright: Elsevier Science.)

where A is the surface area of the particle on which ions may impinge (m^2); n_s is the saturation charge; θ_0 is the greatest angle of region from z axis (rad).

This expression agrees well with measured charging rates.

Representative saturated particle charge as a function of particle radius is presented in Figure 3.

Chemical Conditioning

Conditioning can enhance collection efficiency by reducing resistivity to prevent back corona, increasing cohesivity of the collected layer, enhancing the electric field by increasing the space charge contribution (see below), and increasing agglomeration of small particles. Some exhaust gas conditioning methods which have been used to enhance ESP performance are cooling by in-leakage of cold air, heat exchange to a waste heat boiler, evaporative spray, and chemical

conditioning. The latter has proven most popular in utility applications.

Most commonly, sulfur is combusted and the SO_2 produced is catalytically converted to SO_3 . On combination with the combustion exhaust, SO_3 hydrolyses to produce H_2SO_4 , sulfuric acid. The acid deposits efficiently on fly ash particles, decreasing the particle surface resistivity. SO_3 is added at levels of 1–10 ppm; up to 30 ppm can be added without significant increase in sulfur emission from the ESP. Significant SO_2 is produced on combustion of even low sulfur coal, but only about 1% is converted to the useful SO_3 . Knowledge of the importance of SO_3 was initially gained through experience with conditioning of smelter dusts by sulfide ores.

Ammonium salts were found to be effective when H. J. White was consulted on the problem of decreased ESP efficiency which resulted from a change in petroleum cracker catalyst. He found that replacing ammonia, released by the initial catalyst,

recovered ESP performance. As NH_3 increases collection efficiency with both low and high resistivity boiler ash, and may or may not decrease resistivity, it is thought that this conditioner functions by furnishing salt particles which increase the space charge contribution to the electric field and, by increasing dust cohesiveness, reduce rapping losses.

Characteristics of the Corona Discharge

As voltage applied to a wire discharge electrode is increased, visible discharge points, 'tufts', begin to appear dispersed along the wire. Eventually the tuft pattern stabilizes, appearing as fingers which elongate and retract at 1–10 Hz and remain at somewhat fixed locations along the wire. This stabilization of the corona is indicated by a distinct increase in the slope of the electric field vs. applied voltage curve (Figure 4). Peek determined a semi-empirical expression for the corona onset voltage (V_c) in air:

$$V_c = 3 \times 10^6 am\delta(1 + 0.03\sqrt{\delta/a})\ln(b/a)$$

where V_c is the corona onset voltage (V); a is the radius of discharge electrode (m); m is the wire roughness factor (0.5–0.9); δ is the relative air density; P is the air pressure (Pa).

This discharge produces a current density (with respect to the area of the collector electrode) in the order of 150 nA cm^{-2} . While the ionic composition of the interelectrode space has not been well studied, ionization properties indicate that this current is carried by oxygen, sulfur dioxide, and water, which are negatively charged by the electron current

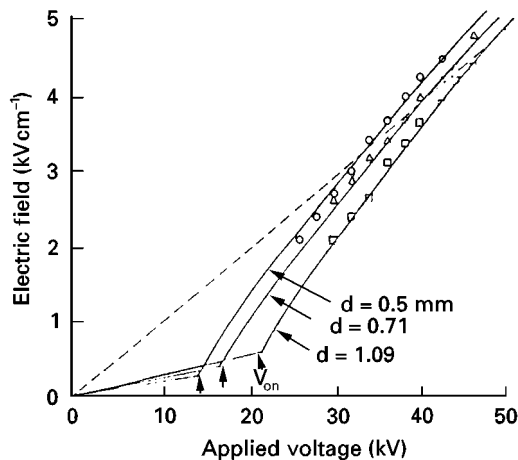


Figure 4 Electric field on the collector electrode just under the corona wire as voltage is applied; d , discharge electrode diameter. $2D = 20 \text{ cm}$; \circ , $d = 0.5 \text{ mm}$; \triangle , $d = 0.71 \text{ mm}$; \square , $d = 1.09 \text{ mm}$. (Reproduced with permission from Ohkubo *et al.* 1985.)

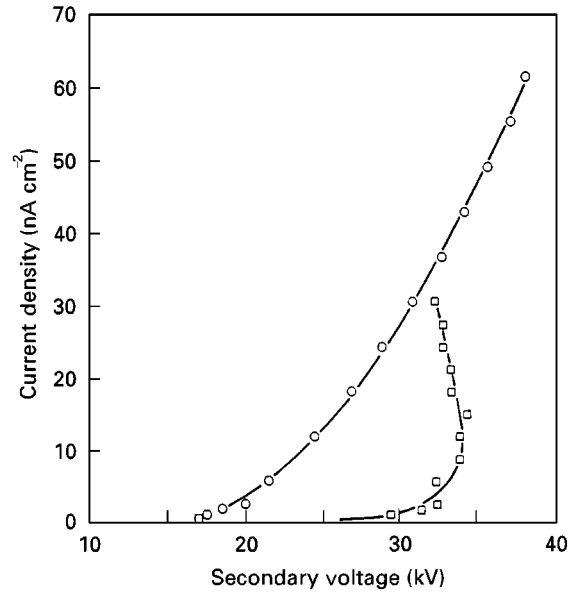


Figure 5 Pilot ESP V-I curves before and after development of severe back corona. \circ , 1 hour after startup; \square , 8 days after startup. (Reproduced with permission from DuBard and Nichols 1990.)

near the corona, and by particles ionized by these primary ions.

The Electric Field

Current vs. voltage curves (Figure 5) are commonly used in monitoring the operation of ESP. For best collection efficiency, ESP units are operated at the maximum voltage which produces a stable current. A discussion of operation monitoring of ESPs is given by DuBard and Nichols.

Much effort has been given to the task of determining the electric field within an ESP. Besides the burden of inability to solve known expressions analytically for the field in a wire-plate electrode system, this task is made difficult by uncharacterized changes in the collector electrode as the dust layer collects on it. The advent of high-speed computing has allowed satisfying solution of the field equations for a clean system.

Cristina *et al.* present a modern method of determining the electric field. These researchers use the following expressions for charge and electric potential:

$$\nabla \cdot (\epsilon \nabla \phi) = -Q$$

$$\nabla \cdot (Q \nabla \phi) = 0$$

where ϵ is the permittivity of air ($\text{C}^2 \text{ N}^{-1} \text{ m}^{-1}$); Q is the ionic charge density (C m^{-2}); ϕ is the electrical potential (V).

These equations have a unique solution for DC ion flow fields. An iterative numerical procedure

is used to balance the electric field and charge density of elements in an array of triangular elements superimposed on the inter-electrode space. These elements are each specified to have a constant ionic charge density. The contribution of space charge by ionized particulate matter is disregarded in this treatment. In the more dust-laden regions of an ESP, particulate matter is found to alter electric field slightly.

Equipotential field maps developed by this treatment show a fairly linear decrease in potential from the discharge to the collector electrode, with circular fields to about one-third distance across the channel (from 57.5 kV to 20 kV), then equipotential field lines parallel to the collector. Near the collector electrode, at about five-sixths the channel width, the potential has decreased to 5 kV. Electric fields of adjacent discharge electrodes interact, producing bell-shaped electric field patterns radiating from each wire to the adjacent collector plates.

Back Corona

In working ESPs, a portion of the applied potential is dropped across the resistive layer of the collected dust. As the dust layer thickens the resistance, hence voltage drop, across the layer increases. If the dust resistivity is high ($\rho > 10^{10} \Omega\text{-cm}$), eventually the field becomes great enough to cause electrical breakdown of gas within the dust layer, generating a back corona. Electrons are ripped from the gas, and the resulting positive ions flow into the inter-electrode space, where they attach to negatively charged particles. The diminished net charge of the particulates leads to greatly diminished collection efficiency; re-entrainment also occurs. A back corona occurs with an electrical field strength across the dust layer (resistance of layer times current) of $8\text{--}12 \text{ kV cm}^{-1}$.

A back corona can be visually observed as a glow on the collection surface. It is also characterized by an increase in corona onset voltage followed by an increase in current for a given applied voltage as compared with a correctly functioning system (Figure 5). The dust layer acts as a resistive-capacitative element in having a lag time before discharge. Both intermittent and pulse energization take advantage of this lag time to allow the application of high voltage without the occurrence of back corona.

Current Density

The electric field at ESP collection surfaces is not uniform due to both the electrode-collector geometry and to irregular resistance resulting from uneven dust layer thickness. The parameter determined in studying the situation at the collection surface is current

density, j (nA cm^{-2}). With poor distribution of current over the dust layer, collection efficiency is diminished. Re-entrainment can occur in regions of low current density, and high local currents can lead to back corona even with a low average current. Landham *et al.* measured the current density distribution in a pilot scale ESP by inserting a segmented copper electrode sensor board into a collector electrode. Conventional, intermittent, and pulse energization with both wire and barbed-strip discharge electrodes were investigated. (Barbed-strip electrodes are used by some manufacturers to force a more uniform current distribution at the collector.)

Intermittent energization (IE) is achieved by interrupting the rectifier circuit output for one to twenty half cycles of the supply power line. A baseline voltage is maintained, with relatively broad pulses superimposed. In pulse energization (PE), pulses of $1 \mu\text{s}$ to 1 ms width and up to -75 kV are superimposed on a DC voltage set just below the 'spark limit'. Both techniques have been found to save energy and to reduce the incidence of back corona. PE is more effective in countering problems with low resistivity dust. Dubard and Nichols set IE to one full AC cycle on and four off (duty cycle 0.2), and PE base voltage -20 kV with 50 Hz , $\sim 125 \mu\text{s}$ width pulses of -25 kV . Conventional full-wave rectified energization (CE) was set at about -35 kV .

These researchers found that CE and PE give Gaussian current density profiles across the sensor plate surface, while IE gives a more even, but lower magnitude distribution. Under good operating conditions (clean collector surface), PE had less collector area above dust layer breakdown current than CE or IE, with 96% useful area as compared to 83% and 86%, respectively. Under severe back corona conditions, PE maintained 84% useful area, CE 12%, and IE 54%. Similar results were obtained with both barbed-strip and wire electrodes. The results indicate a linear relationship between the increase in collector area receiving useful values of current density and collection efficiency.

Among alternative discharge electrode designs, barbed plate discharge electrodes appear more effective in producing uniform current distributions (see McKinney and Davidson). This design may also have some advantage with respect to flow turbulence.

Flow

Besides electric field and current density distribution, gas flow is important in ESP performance. ESP flow velocities vary between 0.2 and 2.0 m s^{-1} . Schwab and Johnson suggest an optimum velocity of between

1.22 and 1.52 m s⁻¹. Lower velocities diminish the turbulent mixing which brings small particles into the low flow region near the collector electrode; higher velocities overwhelm electrostatic attraction of particles to the collector electrode, and can lead to re-entrainment.

Flow within an ESP is inherently turbulent due to high gas flow velocity, which typically results in a Reynolds number of about 10 000 – five times that at which turbulent flow replaces laminar flow. Turbulence in ESPs is complicated by flow obstructions – discharge electrodes and collector stiffening baffles and connectors, and by a non-uniform flow profile at the ESP inlet. At low velocities ($\lesssim 0.5$ m s⁻¹) turbulence resulting from the ion current between discharge and collector electrodes (ionic wind) contributes significantly. The flow regime in an ESP is thus seen to be quite complicated. Baffles within the ESP duct and porous plates at the inlet and outlet are employed to create uniform flow.

Schwab and Johnson have produced a computer model based on Navier–Stokes fluid flow equations as an alternative to traditional reduced scale physical models for flow design. The model can be used to determine inlet plate perforation patterns which produce uniform flow without high flow near the duct walls.

Collection Efficiency

Most important in ESP operation is the particulate collection efficiency, η , the fraction of particulates removed. Around 1920, Deutsch and Anderson independently derived an expression for η , now commonly referred to as the ‘Deutsch equation’:

$$\eta = 1 - \exp\left(-\frac{A}{Q} \omega_e\right)$$

where A is the collector electrode area (m²); Q is the volumetric gas flow rate (m³ s⁻¹); ω_e is the effective particle migration velocity (m s⁻¹).

Efficiency is also expressed as fractional particle penetration, $P = 1 - \eta$. A/Q is the specific collection area (SCA), the parameter of importance in sizing an ESP. Assumptions of the Deutsch equation are that particles are instantaneously fully charged and accelerated, turbulent and diffusive forces cause particles to be distributed uniformly in any cross section of the precipitator, the velocity of the gas stream does not affect the migration velocity of the particles, particle motion is governed by viscous drag where Stokes’ Law applies, the effect of collision between ions and neutral gas molecules can be neglected, and there are

no disturbing effects such as erosion, re-entrainment, uneven gas flow distribution, sneakage, or back corona. A number of researchers have adjusted the Deutsch equation to account for neglected factors. Especially questionable is the assumption of complete turbulent mixing (for instance, see Zhibin and Guoquan). The Deutsch model represents one mixing extreme, with the other extreme being laminar flow (no turbulence). The Deutsch model tends to underestimate η for particles with diameter less than about 1 μ m, and overestimates the collection of larger particles.

The Matt–Öhnfeldt modification attempts to account for variation in particle size distribution:

$$\eta = 1 - \exp\left(-\frac{A}{Q} \omega_k\right)^m$$

where ω_k is the particle migration velocity (m s⁻¹); m is an exponent which depends on particle size distribution.

An m of 0.5 is commonly used with fly ash or cement dust; increasing values can be used with finer size distributions.

In comparing ESP performance under varying conditions, the migration velocity is more useful than η , being independent of ESP collection area and gas flow rate. An important consideration in using ω values is that migration velocity of large particles decreases at a much lower rate with increasing gas flow (or decreased plate size) than that of small particles, hence though small particles will be less efficiently collected, measured ω can increase with gas flow rate.

Migration of charged particles can be treated theoretically. Hall presents the expression:

$$\omega = \frac{4\pi\epsilon_0 k a E_0 E_p C D f}{6\pi\eta} \alpha$$

where k is $3\epsilon/(\epsilon + 2)$; ϵ is the dielectric constant of ash (C N⁻¹ m⁻¹); E_0 is the particle charging electric field strength (V m⁻¹); E_p is the particle collecting electric field strength (V m⁻¹); a is the particle radius (m); C is the Cunningham slip correction; D is the factor to account for diffusion charging of fines; f is the factor accounting for gas turbulence and free electron charging; η is the gas viscosity (Pa s); α is the fractional particle saturation charge.

C is used to adjust diffusion of particles with size comparable to mean-free path of gas molecules. The reader can understand that empirical estimation of ω values, from measured efficiency, is often more productive than theoretical estimation.

The Deutsch model is often used in determining a minimum specific collection area in sizing precipitators. Extrapolation from performance of pilot or other ESPs should be made only with similar designs and similar dusts.

Computer Modelling

Several comprehensive models of particle collection in wire-plate ESPs are available, including the Southern Research Institute (SRI), Research Triangle Institute Sectional (RTIS), Italian Electricity Board (ENEL), and Electric Power Research Institute (ESPM) models. As an example, the ESPM model will be briefly described (see Lawless and Altman).

In ESPM, the applied voltage for a given current density is first determined for a position directly beneath the wire:

$$V = V_c + E_c r_w \left[z - 1 - \ln \left(\frac{z+1}{2} \right) \right]$$

where E_c is the electric field at wire surface at corona onset (V m^{-1}); r_w is the radius of wire (m) and:

$$z = \sqrt{1 + \frac{j b}{\mu \epsilon_0} \left(\frac{b}{V_w} \right)^2}$$

where b is the wire-plate separation (m); μ is the ion mobility ($\text{m}^2 \text{s}^{-1} \text{V}^{-1}$).

Current densities at other plate locations are calculated as:

$$j(\theta) = j_0 \cos^n(\theta)$$

where θ is the angle from between wire and plate (rad); n is a function of j , 2 (near corona onset) to 4.

Ion mobility is based on that of SO_2 and SO_2^- . Space charge resulting from the charging of particles is treated as an equivalent ion current and used to adjust the operating voltage.

Non-dimensional parameters are used in models to add generality to results and to simplify mathematical treatment. For instance, the initial particle charging rate in an ESP model (ESPM), combining both diffusion and field charging, is:

$$\frac{dv}{d\tau} = \frac{3w}{4} \left(1 - \frac{v}{3w} \right)^2 + 1$$

where v is the non-dimensional charge; τ is the non-dimensional exposure time; w is the non-dimensional electric field.

Intermediate and saturation charging rates are modelled by different expressions. Back corona charging can be modelled with ESPM, though better understanding of this process is needed to assure accurate results.

Particle collection is modelled with a modified Deutsch expression:

$$P = \left(1 - \frac{\omega A/Q}{Nw} \right)^{Nw}$$

Nw is a parameter to adjust for turbulence: a high value approaches Deutschian total mixing, a low value approaches laminar collection (laminar when $Nw = 1$). To correct for uneven gas flow, penetration is calculated at several gas velocities and the results combined by weighted averaging. Rapping loss can be specified or estimated by applying conventional dynamics to the falling of agglomerated 'cake' during collector cleaning. The model treats each ESP section separately, 'remixing' particulates exiting from each section.

ESPM can be used to predict V-I curves, 'grade efficiency' (penetration as a function of particle diameter), and other aspects of ESP performance under varying conditions.

Innovative ESP Designs

Several new means have been developed to facilitate collection of submicron and highly resistive particles by ESPs.

Pulse energization is discussed above (see Current density). By superimposing a brief, high voltage pulse on a DC voltage set just below the back corona level, efficient fine particle charging and collection are obtained with highly resistive dusts.

Enhanced particle agglomeration can also facilitate fine particle collection. For instance, Kanazawa *et al.* have accentuated particle agglomeration with a precharging section, in which the gas stream is divided and particles in the two sub-streams given either a positive or a negative charge. On recombining the sub-streams, particles agglomerate through electrostatic attraction. Watanabe *et al.* have devised an alternative method utilizing a three sector design. Large particles are removed in the first ESP sector. A 'modified quadrupole' electrode system in the second sector applies an AC field to enhance particle collision, hence agglomeration. The third section is again a conventional ESP, which removes the agglomerated particles.

Fabric filtration is the surest means of removing fine particles. EPRI has devised the 'Compact Hybrid Particulate Collector' (COHPAC). This design simply places a baghouse after an ESP. The ESP removes much of the particulates, easing the load on the baghouse, hence reducing maintenance. The baghouse reduces pollution due to rapping loss, and is insensitive to changes in fuel.

EPRI has also developed an 'EPRICON' process which can replace conventional chemical conditioning of fly ash from low sulfur coals. In this process, a portion of the gas stream is diverted to a vanadium oxide-based catalytic unit, which efficiently converts SO_2 to SO_3 . Recombination of the treated stream with the bulk results in the necessary conditioning of the fly ash.

See also: **Particle Size Separation:** Hydrocyclones for Particle Size Separation; Sieving/Screening.

Further Reading

Busby HGT and Darby K (1963) Efficiency of electrostatic precipitators as affected by the properties and combustion of coal. *Journal of the Institute of Fuel* 36(268): 184.

Dubard JL and Nichols GB (1990) Diagnosis of electrical operation of electrostatic precipitators. *Journal of Electrostatics* 25: 75.

Hart BR, Powell MA, Fyfe WS and Ratanasthien B (1995) Geochemistry and mineralogy of fly-ash from the Mae Moh lignite deposit, Thailand. *Energy Sources* 17: 23.

Kanazawa S, Ohkubo T, Nomoto Y and Adachi T (1993) Submicron particle agglomeration and precipitation by using a bipolar charging method. *Journal of Electrostatics* 29: 193.

Landham EC Jr., Dubard JL and Piulle W (1990) The effect of high-voltage waveforms on ESP current density distributions. *IEEE Transactions on Industry Applications* 26(3): 515.

McKinney PJ, Davidson JH and Leone DM (1992) Current distributions for barbed plate-to-plane coronas. *IEEE Transactions on Industry Applications* 28(6): 1424.

McKean KJ (1988) Electrostatic precipitators. *IEE Proceedings Pt. A*. 135(6): 347.

Oglesby S Jr. and Nichols GB (1978) *Electrostatic Precipitation*. New York: Marcel Dekker Inc.

Tachibana N (1989) Back discharge and intermittent energization in electrostatic precipitation of fly ash. *Journal of Electrostatics* 22: 257.

Watanabe T, Tochikubo F and Koizumi Y *et al.* (1995) Submicron particle agglomeration by an electrostatic agglomerator. *Journal of Electrostatics* 34: 367.

Zhibin Z and Guoquan Z (1994) Investigations of the collection efficiency of an electrostatic precipitator with turbulent effects. *Aerosol Science and Technology* 20: 169.

Field Flow Fractionation: Electric Fields

S. N. Semenov, Institute of Biochemical Physics,
Russian Academy of Science, Moscow, Russia

Copyright © 2000 Academic Press

Introduction

Field flow fractionation (FFF) represents a class of separation techniques, which use a force field perpendicular to the direction of separation to control the longitudinal velocity of particles injected into the system. It is achieved by particle redistribution in the flow with a parabolic velocity profile due to the action of a transverse force. This transverse force may be due to an electric field, a centrifugal or gravity field, etc. In electric FFF (ElFFF), the transverse movement of the particles is caused by an electric field. The transverse particle velocity, U , is defined by

the expression:

$$U = b \cdot E \quad [1]$$

where b is the particle electrophoretic velocity, and E is the electric field strength in the channel interior, which is available both for the particles and the flow of the carrier liquid. The particle electrophoretic mobility is related to the particle electrokinetic potential (zeta-potential):

$$b = \frac{\varepsilon \zeta}{4\pi\eta} f\left(\frac{R}{\delta}\right) \quad [2]$$

where ε is the dielectric constant of the carrier liquid, η is the carrier liquid viscosity, ζ is the particle electrokinetic potential, R is the particle diameter, and δ is the Debye length characterizing the screening